JOURNAL OF VIROLOGY, Mar. 2004, p. 2510–2516 Vol. 78, No. 5
0022-538X/04/$08.00+0 DOI: 10.1128/JVI.78.5.2510–2516.2004
Copyright © 2004, American Society for Microbiology. All Rights Reserved.

A Virulence Factor of Myxoma Virus Colocalizes with NF-κB in the Nucleus and Interferes with Inflammation

Christelle Camus-Bouclainville,[1] Laurence Fiette,[2] Sophie Bouchiha,[2] Béatrice Pignolet,[1] Dorian Counor,[1] Cédric Filipe,[1] Jacqueline Gelfi,[1] and Frédérique Messud-Petit[1]*

UMR 1225 Interactions Hôtes Agents Pathogènes, INRA/ENVT, Ecole Nationale Vétérinaire de Toulouse, 31076 Toulouse Cedex,[1] and Unité d'Histopathologie, Institut Pasteur, 75724 Paris Cedex 15,[2] France

Received 4 August 2003/Accepted 3 November 2003

NF-κB is one of the most important elements that coordinate stress-induced, immune, and inflammatory responses. *Myxoma virus*, a member of the *Poxviridae* family responsible for rabbit myxomatosis, codes for several factors that help its survival in the host. In this study, we focused on the product of the M150R gene. We show that the protein has nine ankyrin repeats (ANKs), with the eighth having a close similarity with the nuclear localization signal-containing ANK of I-κBα, which regulates NF-κB activity by sequestering it in the cytosol. Because the viral protein is targeted to the nucleus, it was named MNF, for myxoma nuclear factor. This localization was lost when the eighth ANK was removed. In tumor necrosis factor alpha-treated cells, MNF and NF-κB colocalized as dotted spots in the nucleus. In vivo experiments with a knockout virus showed that MNF is a critical virulence factor, with its deletion generating an almost apathogenic virus. Detailed histological examinations revealed an increase in the inflammatory process in the absence of MNF, consistent with the interference of MNF with the NF-κB-induced proinflammatory pathway. Because MNF has homologs in other poxviruses, such as vaccinia, cowpox, and variola viruses, this protein is probably part of a key mechanism that contributes to the immunogenic and pathogenic properties of these viruses.

Inflammation is a very efficient way to get rid of invaders such as viruses. Poxviruses, among the largest DNA viruses, have become a model for host-virus interactions. This is due to their ability to "play" with the host, disrupting most, if not all, pathways of the antiviral response, including the inflammatory reaction. A striking effect of poxviruses on the host response was described recently by Oie and Pickup (17), who demonstrated that some members of the *Orthopoxvirus* genus could interfere with the regulation of NF-κB activation. By specifically targeting NF-κB, orthopoxviruses access the core of multiple immune processes.

Myxoma virus (MV), a member of the *Poxviridae* family responsible for rabbit myxomatosis, has a particular talent for escaping or subverting the host artillery. MV has a double-stranded DNA genome of 162 kbp (4), with a central region containing highly conserved enzymatic and structural genes required for the maintenance of essential viral functions. Peripheral regions of the DNA, within and near the inverted terminal repeats (ITRs) at both sides of the genome, encode nonessential factors that contribute to the modulation of the host response to infection. These factors include serpins (serine proteinase inhibitors), such as SERP1 (30), Serp2 (14, 18), and Serp3 (9), and a scrapin (8), responsible for major histocompatibility complex class I downregulation by MV, all of which are located near the right end of the genome. Several other genes present in the same region have functions that are still speculative. Here we show the functional characterization of M150R, a gene whose product localizes to the nucleus of the cell, which led us to tentatively name the protein myxoma nuclear factor (MNF). MNF possesses ankyrin (ANK) repeats, which are thought to be involved in protein-protein interactions. Our data suggest that MNF is implicated in the subversion of the NF-κB activation pathway.

* Corresponding author. Mailing address: UMR 1225, Ecole Nationale Vétérinaire de Toulouse, 23 chemin des Capelles, 31076 Toulouse Cedex, France. Phone: (33) 561-19-38-78. Fax: (33) 561-19-39-74. E-mail: f.messudpetit@envt.fr.

MATERIALS AND METHODS

Cells and viruses. Rabbit kidney cells (RK13) were maintained in Dulbecco's minimum essential medium supplemented with 10% fetal calf serum. The wild-type strain T1 and the MV-ΔMNF mutant of MV were grown in rabbit kidney cells (RK13) in OPTI minimum essential medium supplemented with 2% fetal calf serum. Strain T1 of MV is a field strain that was isolated in Toulouse, France, with a biology and a life cycle comparable to those of the Lausanne strain (3). Baby Green monkey kidney cells (BGMK) were maintained in Dulbecco's minimum essential medium with 10% calf serum. Subconfluent layers of BGMK cells were grown on glass coverslips and transfected with plasmids encoding green fluorescent protein (GFP) fusions by use of liposomes (Lipofectamine; Gibco BRL). At 24 h posttransfection, cells were rinsed twice with phosphate-buffered saline (PBS) for subsequent use in confocal microscopy.

Cloning, sequencing, and computer analysis of DNA and protein sequences. The viral DNA upstream of *serp2* (M151R) was amplified and sequenced as described previously (9). DNA sequences were analyzed with DNA Strider 1.3 software (13) and the BLAST program (GenBank). Searches for ANK repeats were performed with the REP (1), PFSCAN (6), and SMART (11, 23) online software packages.

Construction of GFP fusions. GFP-MNF fusions were obtained by using the pEGFP-F plasmid vector (BD Biosciences-Clontech), which contains a jellyfish GFP gene optimized for maximum fluorescence downstream of a cytomegalovirus promoter. A pEGFP-MNF plasmid was engineered by amplifying the M150R open reading frame by PCR using primers 5′-*Bgl*II-GFP-M150R (5′-GGAAGATCTGTATTCGACCCGTTACACGA-3′) (the *Bgl*II site is underlined) and 3′-*Pst*I-GFP-MNF (5′-AACTGCAGCTTGAAAAGCTCCATAATCG-3′) (the *Pst*I site is underlined). The resulting PCR fragment was inserted between the *Bgl*II and *Pst*I sites in pEGFP-F, thus replacing the farnesylation box-coding sequence downstream of the GFP sequence. pEGFP-MNFΔANK8 was constructed by using the following sets of primers: (i) forward primer 5′-*Bgl*II-GFP-M150R paired with reverse primer 5′-TCCCATATGGATGTAATCCACACTTGTGATAGATTTATG-3′, which corresponds to nucleotides (nt) 869 to 853 fused to nt 753 to 727 of M150R, and (ii) forward primer 3′-*Pst*I-GFP-M150R paired with reverse primer 5′-CTATCACAAGTGTGGATTACATCCATATG

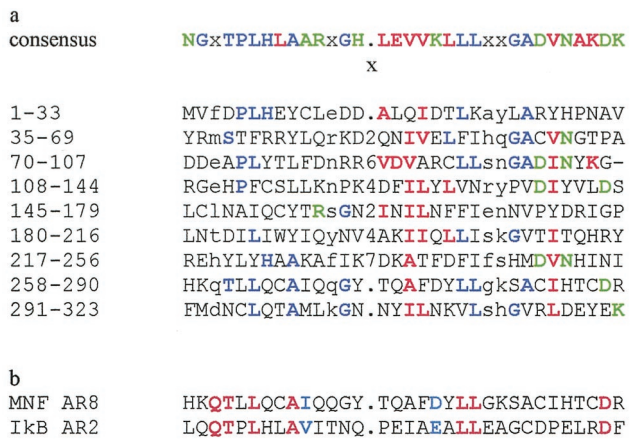

FIG. 1. MNF ANK repeats. (a) Alignment of MNF ANK repeats with a consensus (15): blue, well-conserved residues; red, semiconserved residues (same type); green, semiconserved residues (different types); and black, nonconserved residues. Residue position marked "x" below the consensus sequence accepts 0 to 9 amino acids. (b) Alignment of MNF eighth ANK repeat with 1-κB second ANK repeat: red, identical residues; and blue, similar residues.

GGAAAAGATAAAATC-3′, which corresponds to nt 739 to 753 fused to nt 853 to 876 of M150R. Both PCR products were purified and mixed in the presence of *Taq* polymerase. Primers 5′-*Bgl*II-GFP-M150R and 3′-*Pst*I-GFP-M150R were then used to generate the M150R gene with a deletion of nt 754 to 852 (33 codons). Cloning into the pEGFP-F vector was performed after digestion with *Bgl*II and *Pst*I. The pEGFP-F farnesylation box-coding sequence was removed by double digestion with *Bgl*II and ligation. The resulting plasmid was referred to as pEGFP.

Confocal microscopy observations. BGMK cells were plated into LabTek multichamber slide flasks (Falcon). At 24 h posttransfection, cells were stimulated for 20 min at 37°C with 15 ng of human tumor necrosis factor alpha (TNF-α)/ml in culture medium, rinsed twice in PBS, fixed for 90 min at room temperature with 4% paraformaldehyde in PBS, and permeabilized with 0.1% Triton X-100 for 30 min at room temperature. Cells were then incubated with rabbit anti-human NF-κB antibodies (1/200; Santa Cruz) in 0.05% Tween in PBS for 1 h at 37°C, rinsed three times in PBS-Tween, and incubated with biotinylated goat anti-rabbit antibodies (1/500; Sigma) for 1 h at 37°C. Cy3-conjugated streptavidin (Jackson ImmunoResearch) was added at a dilution of 1/20,000 in PBS and was incubated for 30 min at 4°C. After three PBS washes, the samples were mounted with PBS-glycerol (1:1) and observed with a confocal LSM Olympus microscope fitted with a 60× Olympus objective.

Construction of MV-ΔMNF recombinant and revertant viruses. For evaluation of the involvement of MNF in MV pathogenicity, the M150R gene was inactivated by deletion of the central 888 bp and replacement with a *lacZ* marker gene in an antisense position. The forward primer M150R-*Fwd* (5′-AATAGTG CGATCTTTGTGCGCTATAGG-3′) was paired with reverse primer M150R-*Rev* (5′-CTCCATAATCGCACTTATACA-3′) to amplify M150R; the PCR fragment was cloned into the pGEM-T vector to generate the pGEM-M150R plasmid. pGEM-M150R was digested with *Eco*RV, which cuts twice in M150R. *lacZ* under the control of the vaccinia virus p7.5 promoter was obtained by digesting the pSC11 plasmid (5) with *Xba*I and *Pst*I, followed by T4 DNA polymerase treatment to create blunt-ended fragments. After ligation, a plasmid with *lacZ* inserted in an antisense position with regard to M150R was selected. This construct was used for the transfection of MV-infected RK13 cells. MV-ΔMNF mutant viruses were screened by their LacZ phenotype in the presence of X-Gal (5-bromo-4-chloro-3-indolyl-β-D-galactopyranoside). A revertant virus, MV-MNF-*rev*, containing a wild-type M150R open reading frame, was obtained by transfecting plasmid DNA containing the complete M150R gene into MV-ΔMNF-infected RK13 cells and by reverse white-blue screening.

RNA extraction and RT-PCR analysis. RK13 cells (5×10^6) were infected at a multiplicity of infection of 5 with wild-type MV or MV-ΔMNF. Total RNAs were isolated at 2, 4, 8, 12, and 16 h postinfection (p.i.) by use of TRIzol reagent (Invitrogen) according to the manufacturer's instructions. In addition, the total RNA was also extracted from 16-h infected cells treated with 40 μg of cytosine arabinoside (AraC)/ml at the time of infection. All RNA samples were subjected to DNase I (Invitrogen) treatment according to the manufacturer's instructions. For reverse transcription (RT)-PCR analysis, an M150R-specific primer was used for cDNA first-strand synthesis, followed by PCR amplification using M150R-specific primers M150R-*Fwd* and M150R-*Rev*, corresponding to the 5′ and 3′ ends of the open reading frame, respectively. A control RT-PCR, in which the reverse transcriptase was omitted during the RT step, was performed with a sample from 8 h p.i.

Infection of rabbits with MV-ΔMNF. Eight-week-old male New Zealand White rabbits were obtained from a local supplier and housed in biocontainment facilities according to the guidelines of the European Community Council on Animal Care (European Council directive 86/609/ECC, 24 November 1986). All procedures on animals were performed by workers accredited by the French Ministry of Agriculture and were aimed at limiting animal pain and distress. Infections were performed intradermally in the right ear with 5×10^3 PFU of either wild-type MV, MV-ΔMNF, or MV-MNF*rev*. Rabbits were monitored daily for clinical signs of myxomatosis (7). Rabbits that became moribund were sacrificed by use of T61 (Distrivet) administered intravenously. For histological studies, nine rabbits were inoculated with MV strain T1 and nine were inoculated with MV-ΔMNF, as described above. At 4, 8, and 12 days p.i., three animals from each group were sacrificed. Two mock-infected rabbits were sacrificed and used as controls.

Histological examination. All animals were subjected to a complete postmortem examination. Tissues from the injection site (primary site, ear) and parotid lymph node were taken and stored in 10% neutral formalin for further analysis. After fixation, tissues were processed routinely into paraffin blocks, sectioned at a 4-μm thickness, and stained with hematoxylin and eosin for microscopic examination. Histologic lesions were assessed and graded as follows: 1, minimal; 2, moderate; 3, severe.

Viral load in tissues. Contralateral parotid lymph nodes were sampled from rabbits infected with either wild-type or MV-ΔMNF mutant virus at 4, 8, and 12 days p.i. and were frozen at −80°C; after thawing, tissues were further disrupted by homogenization in Dulbecco's minimal essential medium. Virus titers in the different samples were determined by standard plaque titration on RK13 cell monolayers.

RESULTS

Sequence analysis. M150R codes for one of the four ANK repeat-containing proteins encoded by the genome of MV (4). A REP analysis (1) of the M150R protein revealed six repeats above the threshold, at amino acids (aa) 35 to 69, 70 to 107, 145 to 179, 180 to 216, 258 to 290, and 291 to 323. SMART (11, 23) identified four of the above repeats (aa 70 to 107, 180 to 216, 258 to 290, and 291 to 323) and another one (aa 108 to 144). Taken together, these data identify seven ANK repeats.

However, Bork (2) indicated that ANK repeats with weak signals can be added manually when they either occur between clearly defined repeats or correspond to less-conserved terminal repeats. Applying these criteria to the M150R sequence allows the identification of two additional divergent ANK repeats, one at the N terminus (aa 1 to 34) and one in the middle of the sequence (aa 217 to 256). Thus, up to nine tandem ANK repeats can be identified in the M150R protein sequence from aa 1 to 323. Figure 1a shows a tentative alignment of the repeats with a consensus sequence (15).

The DNA upstream of the ATG was previously described (4) to be consistent with the expression of M150R as an early gene.

Expression of M150R RNA in MV-infected cells. RT-PCR analysis of total RNA purified from wild-type MV-infected cells demonstrated that the MNF transcript was detectable as early as 4 h postinfection and could still be detected at 16 h postinfection, even in the presence of AraC, an inhibitor of DNA replication and thus of late gene expression (Fig. 2). These results indicate that MNF is expressed as an early and

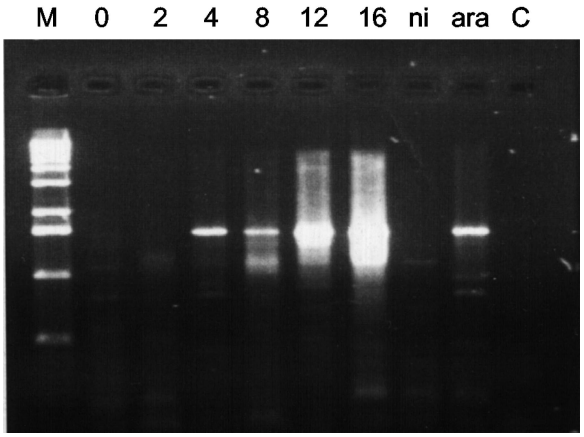

FIG. 2. Expression of M150R mRNA in infected cells. mRNAs were extracted and subjected to RT-PCR using primers specific for M150R. Lane M, marker; lanes 0 to 16, hours postinfection with wild-type MV; lane ni, mock-infected cells; lane ara, cells infected with wild-type MV for 12 h and treated with AraC at the time of infection; and lane C, control without reverse transcriptase.

relatively stable mRNA, consistent with the sequence analysis of the promoter region.

Cellular localization of the protein. To determine the subcellular localization of the protein, we used a plasmid expressing a GFP-MNF fusion (with MNF fused downstream of GFP) to transfect RK13 cells. Twenty-four hours after transfection, the cells were examined by fluorescence under a confocal microscope. As shown in Fig. 3, a punctate nuclear pattern was observed with the GFP-MNF fusion at 24 h posttransfection, in contrast to the diffuse (cytoplasmic and nuclear) pattern of GFP alone. This result was striking, since no classical nuclear localization signal (NLS) had been identified in the MNF sequence. However, it has already been shown that an ANK repeat can be used as an NLS. Such is the case for I-κBα, the second ANK repeat of which is responsible for its nuclear translocation (21).

To determine whether MNF nuclear translocation was also due to one of its ANK repeats, we engineered a GFP-MNF fusion with a deleted of its eighth ANK repeat (GFP-MNFΔANK8), which proved to be closest in similarity to the NLS-containing one of I-κBα (Fig. 1b). As shown in Fig. 3, deletion of the eighth ANK repeat of MNF prevented translocation to the nucleus.

MNF is essential to MV pathogenicity. To evaluate the role of MNF in the pathobiology of MV, we inoculated European rabbits intradermally with either MV strain T1, MV-MNF*rev*, or MV-ΔMNF. The clinical course was monitored daily for 28 days. There was a dramatic reduction in the virulence of MV-ΔMNF compared to that of the wild type or MV-MNF*rev* in rabbits (Table 1).

At day 4 p.i., all animals had developed a lesion at the inoculation site (primary myxoma) which seemed to be more inflamed, congested, and exudative for rabbits inoculated with the MV-ΔMNF virus.

At day 8 p.i., secondary myxomas appeared on the faces and ears of rabbits inoculated with the wild-type MV or MV-MNF*rev*. These animals also suffered from moderate respiratory infections and were less active. In contrast, of the 12 rabbits inoculated with the MV-ΔMNF virus, only 3 had secondary myxomas, which were very small and rare. No respiratory signs were noted. Only one rabbit had a mild blepharitis.

At day 12 p.i., the rabbits inoculated with the wild-type MV had developed multifocal secondary myxomas which were turning necrotic. They had developed severe infections of the respiratory tract, were prostrated, and therefore were euthanized for ethical considerations. Animals that had been injected with the MV-ΔMNF mutant had very small secondary myxomas, restricted to the face and ears. None of the animals which had received the MV-ΔMNF mutant suffered from respiratory infections, and they continued regular activities. All of them had a discrete inflammation of the testicles.

At day 21 p.i., all of the rabbits inoculated with the MV-ΔMNF mutant had recovered. At day 28 p.i., they were resistant to a challenge with wild-type strain T1.

To summarize, our clinical observations revealed that infection with an MV-ΔMNF mutant virus induced a delay in the

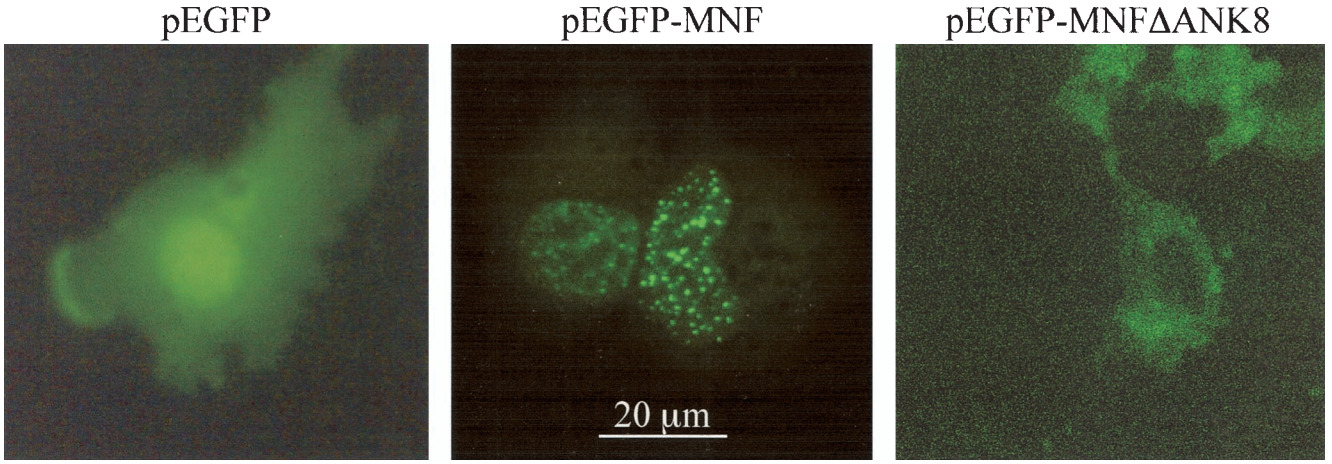

FIG. 3. Cellular localization of MNF. RK13 cells grown on coverslips were transfected with expression vectors for GFP-tagged versions of MNF. Cells were fixed at 24 h posttransfection. Left panel, GFP control; center panel, GFP-MNF; right panel, GFP-MNFΔANK8.

TABLE 1. Pathogenicity of MNF in European rabbits

Day	Procedure, symptom(s), or result	
	Wild-type MV and MV-MNF*rev*[a]	MV-ΔMNF[b]
0	Intradermal inoculation of four rabbits with 5,000 PFU of wild-type MV strain T1 and of four rabbits with 5,000 PFU of MV-MNF*rev*	Intradermal inoculation of 12 rabbits with 5,000 PFU of MV-ΔMNF
4	Primary lesions at inoculation sites (soft, congested, and ca. 1 cm)	Primary lesions at inoculation sites (raised, soft, congested, ca. 1.5 cm); one rabbit showed mild blepharitis
8	Large and diffused primary myxomas, gram-negative bacterial infections of conjunctivas and respiratory tracts, dyspnea, and multiple secondary myxomas on faces and ears	Congested, exudating (ca. 2 cm) primary myxomas, three rabbits with a few (1 to 3) minute myxomas on the nose; blepharitis in the one rabbit healed, leaving only a minute myxoma
12	Multiple secondary myxomas, turning necrotic, dyspnea, severe infections of respiratory tracts, prostrated and emaciated animals, severe inflammation of the testicles; all rabbits were sacrificed because of the increased severity of symptoms	Flat primary myxomas, topped by a crust, minute myxomas on ears, noses, and eyelids of all rabbits; no dyspnea or inflammation of the respiratory tract was seen. Discrete inflammation of the testicles
21		Scabbed primary myxomas, involuted secondary myxomas; all rabbits recovered
28		All rabbits were resistant to challenge with wild-type MV strain T1

onset of cutaneous secondary myxomas as well as a reduction in their size. Only a discrete inflammation of the testicles was observed, and no respiratory infection was detectable, resulting in a striking rate of recovery (100% in our hands), compared to the systematically fatal course after infection with the wild-type MV.

Histological analysis of lesions from wild-type MV- and MV-ΔMNF-infected rabbits. We performed a detailed histological examination of tissue materials from the primary infection site (ear) at various times during the course of infection. At day 4 p.i., there were moderate edema, hemorrhaging, and mucinosis in the epidermis for both groups of rabbits. However, the nature of the cells in the lesions differed significantly between the two groups (Fig. 4): whereas heterophils were present in both groups, the majority of cells in rabbits infected with the MV-ΔMNF mutant were mononuclear cells. At day 8 p.i., there were marked mucinosis, edema, and hemorrhaging at the site of infection with the wild-type MV; in these lesions, most cells still consisted of heterophils; in rabbits infected with the MV-ΔMNF mutant, a mononuclear cell infiltrate was present and heterophils were almost absent. At day 12 p.i., the infiltration by heterophils, which had been regularly increasing in rabbits infected with the wild-type MV, had reached its maximal intensity. Mononuclear cells also had infiltrated the lesion, but they were a minority. In rabbits infected with the MV-ΔMNF mutant, the lesions had almost completely regressed and consisted quasiexclusively of mononuclear cells.

Significant differences were observed in the parotid lymph nodes (Table 2): at day 4 p.i., there were a moderate paracortical hypoplasia and a moderate infiltration of heterophils in rabbits infected with the wild-type MV. With the MV-ΔMNF mutant virus there were a minimal paracortical hyperplasia and a minimal heterophilic infiltration; syncytia were observed. At day 8 p.i., with the wild-type MV there were a moderate infiltrate of histiocytes and heterophils and a severe periadenitis; secondary myxomas were observed. With the MV-ΔMNF mutant virus, there were a moderate paracortical hyperplasia, a severe follicular hypoplasia, a moderate infiltrate of histiocytes, a minimal infiltration of heterophils, and no periadenitis; secondary myxomas were absent. At day 12 p.i., with the wild-type MV there was a severe periadenitis, a severe follicular hypoplasia, a minimal paracortical hyperplasia, and multiple secondary myxomas. With the MV-ΔMNF mutant virus, there was a minimal periadenitis, a moderate follicular hypoplasia, a severe paracortical hyperplasia, and no myxomas. Syncytia were observed in both groups.

From these observations, we conclude that infection with the MV-ΔMNF mutant virus results in an inflammatory process at the site of injection which is more rapidly progressive and resolves more quickly than that with the wild-type MV;

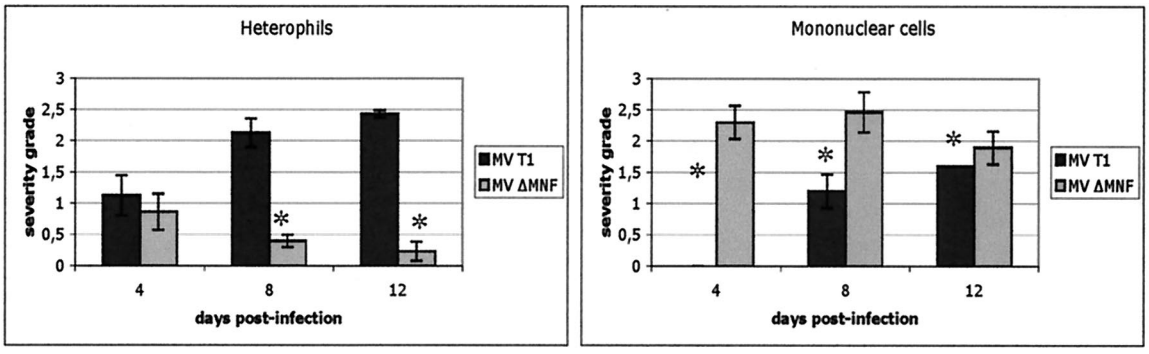

FIG. 4. Inflammatory infiltrates at the primary site of infection. Rabbits were infected with the wild-type (T1 strain) or MV-ΔMNF mutant virus. The severity grade corresponds to the mean of the number of inflammatory cells at 10 time points for the sample. Asterisk, $P < 0.05$ (Mann-Whitney test).

TABLE 2. Histological observations of lesions from rabbits infected with wild-type MV or MV-ΔMNF mutant virus

Symptom	Lesion intensity[a] with the indicated virus at:					
	day 4 p.i.		day 8 p.i.		day 12 p.i.	
	Wild-type	ΔMNF	Wild-type	ΔMNF	Wild-type	ΔMNF
Perivascular dermatitis[b]						
Edema	++	++++	+++	++	++++	+++
Heterophils	++	++	+++	+	++++	+
Mononuclear cells		++	+	+++	++	++
Lymphadenitis						
Paracortical hypoplasia	++					
Paracortical hyperplasia		+	+	++	+	+++
Follicular hypoplasia	+	+	++	+++	+++	++
Sinusal histiocytosis			++	++	+	++
Infiltration by heterophils	++	+	++	+		
Periadenitis			+++		+++	+
Secondary myxomas			++		++	
Syncytia		+		++	+	++

[a] Lesion intensity: +, minimal; ++, moderate; +++, severe.
[b] Samples were taken from lesions at the inoculation sites.

whereas the MV-ΔMNF mutant virus induces an early and subacute lymphadenitis, infection with the wild-type MV results in a massive lymphoid destruction by myxomas.

Virus load in tissues. To show that the differences found during the clinical course of the disease and the histological results between both virus infections were not associated with an impairment of the MV-ΔMNF mutant virus to replicate in vivo, we measured the virus load in the parotid lymph nodes of rabbits infected with either the mutant or the wild-type MV. At day 12 p.i., no significant difference could be found between both viruses (data not shown). We thus conclude that the ability of MV-ΔMNF to replicate in vivo is not affected and cannot explain the observed attenuated phenotype.

Interference with NF-κB. In order to determine whether MNF interferes with inflammation through an NF-κB-dependent pathway, we observed its effect on NF-κB localization with or without TNF-α stimulation. BGMK cells were transfected with a plasmid expressing either GFP alone, GFP-MNF, or GFP-MNFΔANK8. Twenty-four hours after transfection, cells were either stimulated with TNF-α or left unstimulated, stained for NF-κB p65, and examined by immunofluorescence under a confocal microscope. The cytoplasmic localization of p65 in untreated cells was not affected upon transfection with pEGFP-MNF (Fig. 5c). In TNF-α-induced cells, p65 was translocated to the nucleus whether MNF was present or not (Fig. 5f and g). However, the nuclear translocation of p65 was associated with a punctate pattern associated with its colocalization with MNF in pEGFP-MNF-transfected cells (Fig. 5d to f). Transfection with pEGFP or pEGFP-MNFΔANK8 did not affect p65 distribution, which was not associated with MNFΔANK8 upon stimulation with TNF-α (data not shown).

DISCUSSION

This study demonstrates that the M150R gene of MV is expressed as an early gene, with an mRNA that is relatively stable throughout the viral cycle. The M150R product contains up to nine potential ANK repeats, although previous reports had predicted only five of them (4). M150R has homologs in orthopoxviruses, such as vaccinia, cowpox, and variola viruses (25, 26). For these viruses, as well as for MV, predictions suggested that the protein is cytoplasmic.

However, when expressed by transfection, the protein of MV localizes in the nucleus with a punctate pattern. This nuclear localization led us to name this protein myxoma nuclear factor. A multitude of different roles have been assessed for ANK repeat proteins, which can be found in the nucleus, the cytoplasm, or the extracellular milieu (24). The best documented feature of ANK repeats is the ability to mediate protein-protein interactions. One star among ANK repeat proteins is I-κB, which binds to the transcription factor NF-κB, thus keeping the latter in an inactive I-κB/NF-κB complex. The NLS region of the p65 subunit of NF-κB wraps around and interacts with hydrophobic residues on ANK1 of I-κBα, while ANK2 residues of I-κBα contact NLS residues on the p50 subunit of NF-κB (27). When not bound to NF-κB, I-κBα is constitutively transported to the nucleus through a specific transport process (29). Although no typical NLS is discernible, the nuclear import of I-κBα is mediated by a sequence within its second ANK repeat (21). We have shown that one of the ANK repeats of MNF is used as an atypical NLS, as is the case for the I-κBα protein. The nuclear targeting of MNF is dependent on the presence of the eighth ANK repeat, which is the closest in sequence to the second ANK repeat of I-κBα. However, fusion of the eighth ANK repeat of MNF to GFP was not sufficient to induce the translocation of GFP to the nucleus (data not shown). This might be explained by an incorrect folding of the ANK motif, which might require additional domains that are present on MNF but absent from GFP.

In TNF-α-stimulated cells, NF-κB p65 seemed to colocalize with MNF in the nucleus. Whereas nuclear translocation of p65 is expected after TNF-α stimulation, this punctate pattern is radically different from the rather diffuse localization usually observed for NF-κB. This could mean that MNF traps NF-κB p65 after its entry into the nucleus, thus leading to punctate localization for both proteins. The spot-like redistribution of NF-κB in the presence of MNF argues against coincidental colocalization and is indeed a strong argument towards an interaction between the viral protein and the transcription factor.

To assess the role of MNF in the pathogenesis of myxomatosis, we engineered a fully replication-competent MV mutant with a deletion in the M150R open reading frame. Although the mutant and wild-type viruses seem to replicate at the same level in vivo, the former induced very mild symptoms, with few discrete secondary myxomas, no respiratory infection, normal activity, and very strikingly, no lethality. Histological analysis of the primary myxoma (inoculation site) and parotid lymph node showed that deletion of the M150R gene allowed a more rapid and quickly resolved inflammation. These observations are in accordance with an inhibition of NF-κB-mediated synthesis of proinflammatory cytokines by MNF. Which cytokines are targeted and how they may affect the course of the disease need to be determined. Since MV infects not only fibroblasts, but also T cells, monocytes, and activated macrophages, an impairment of inflammatory reactions at a central checkpoint such as NF-κB would not be surprising. It is noteworthy that the M150R gene is one of the few MV genes which do not have homologs in *Shope fibroma virus*, a *Leporipoxvirus* closely re-

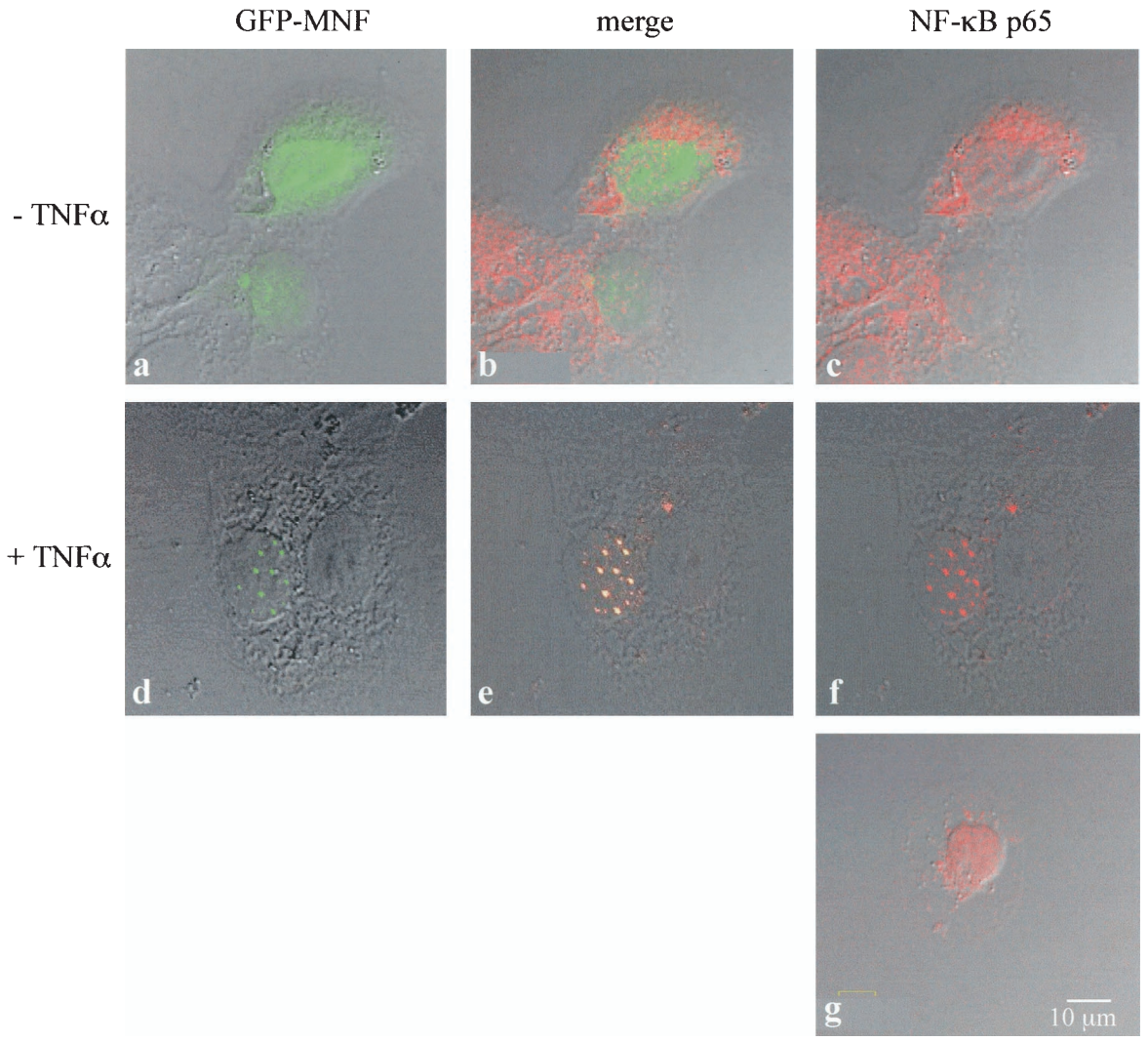

FIG. 5. Colocalization of MNF with p65 in the nucleus. BGMK cells grown on coverslips were transfected with a GFP-MNF-expressing plasmid (a to f) or were left untransfected (g). At 20 h posttransfection, cells were left untreated (a to c) or treated with TNF-α (d to g) for 30 min, fixed, and stained with anti-p65 antibody. Colocalization is shown in yellow in the merge panels.

lated to MV (31). Indeed, Shope fibroma virus infection is characterized by a very strong inflammation that seems to prevent propagation in the host from the infection site.

The NF-κB pathway is an attractive target for viruses which have developed different strategies leading to either activation or inhibition of NF-κB-dependent gene transcription (for a review, see reference 22). Among the viral proteins shown to negatively affect NF-κB function, the African swine fever virus (ASFV) A238L protein contains ANK repeats, with a strong homology with porcine I-κBα (19). The A238L protein is located in the cytoplasm of infected cells, where it binds to NF-κB, thus preventing its translocation to the nucleus (20, 28). This viral protein acts as a surrogate of cellular I-κBα after it is degraded in stimulated macrophages. However, although ASFV is highly pathogenic in domestic pigs, causing an acute hemorrhagic and frequently fatal disease, inactivation of the viral I-κB homolog did not affect virulence in susceptible domestic swine (16). One hypothesis is that because the natural host of ASFV is the warthog and not the domestic pig, the protein performs a host-range-defining function. The European rabbit is the natural host of MV, and the drastic effect of the suppression of MNF on virulence is obviously more easily detectable. However, the in vitro colocalization experiments were performed with BGMK cells, suggesting that MNF might be able to interact with NF-κB even under heterologous conditions.

It has been shown that some orthopoxviruses can interfere with NF-κB activation (17). Although the C9L gene of orthopoxviruses is the equivalent of the M150R gene, the mechanisms described by Oie and Pickup cannot be attributed to the MNF homolog. These authors showed that cowpox virus interferes with NF-κB activation by preventing I-κBα degradation after its phosphorylation on serine residues. Indeed, it appears that, provided that the C9L gene is functional in cowpox virus, there are at least two mechanisms that concur for NF-κB activity repression. This is often the case with large DNA viruses, and poxviruses, in which redundant functions are exerted at various levels, master the subversion of host defense strategies. An alternative mechanism of NF-κB activation, in

which tyrosine but not serine phosphorylation of I-κBα occurs, has been described previously (10). Activation which results in tyrosine phosphorylation of I-κBα can trigger NF-κB activation without I-κBα degradation (12). Although the physiopathological circumstances of the alternative mechanism are not fully understood, it is possible that MNF or its C9L counterpart represents a second barrier, when I-κBα degradation is bypassed, to ensure interference with NF-κB pathways.

The description of a nuclear factor in a family of viruses that are strictly intracytoplasmic is exciting. The ANK repeat features of this factor and its distribution in the nucleus open up possibilities for interactions with other major transcription factors, which are now being investigated.

ACKNOWLEDGMENTS

We thank Josyane Loupias and Brigitte Peralta for excellent technical assistance.

This work was supported by a grant from the Institut National de la Recherche Agronomique.

REFERENCES

1. **Andrade, M. A., C. P. Ponting, T. J. Gibson, and P. Bork.** 2000. Homology-based method for identification of protein repeats using statistical significance estimates. J. Mol. Biol. **298:**521–537.
2. **Bork, P.** 1993. Hundreds of ankyrin-like repeats in functionally diverse proteins: mobile modules that cross phyla horizontally? Proteins **17:**363–374.
3. **Bouvier, G.** 1954. Quelques remarques sur la myxomatose. Bull. Off. Int. Epizoot. **46:**76–77.
4. **Cameron, C., S. Hota-Mitchell, L. Chen, J. Barrett, J. X. Cao, C. Macaulay, D. Willer, D. Evans, and G. McFadden.** 1999. The complete DNA sequence of myxoma virus. Virology **264:**298–318.
5. **Chakrabarti, S., K. Brechling, and B. Moss.** 1985. Vaccinia virus expression vector: coexpression of β-galactosidase provides visual screening of recombinant virus plaques. Mol. Cell. Biol. **5:**3403–3409.
6. **Falquet, L., M. Pagni, P. Bucher, N. Hulo, C. J. Sigrist, K. Hofmann, and A. Bairoch.** 2002. The PROSITE database, its status in 2002. Nucleic Acids Res. **30:**235–238.
7. **Fenner, F., and F. Ratcliff.** 1965. Myxomatosis. Cambridge University Press, Cambridge, United Kingdom.
8. **Guerin, J. L., J. Gelfi, S. Boullier, M. Delverdier, F. A. Bellanger, S. Bertagnoli, I. Drexler, G. Sutter, and F. Messud-Petit.** 2002. Myxoma virus leukemia-associated protein is responsible for major histocompatibility complex class I and Fas-CD95 down-regulation and defines scrapins, a new group of surface cellular receptor abductor proteins. J. Virol. **76:**2912–2923.
9. **Guerin, J. L., J. Gelfi, C. Camus, M. Delverdier, J. C. Whisstock, M. F. Amardeihl, R. Py, S. Bertagnoli, and F. Messud-Petit.** 2001. Characterization and functional analysis of Serp3: a novel myxoma virus-encoded serpin involved in virulence. J. Gen. Virol. **82:**1407–1417.
10. **Imbert, V., R. A. Rupec, A. Livolsi, H. L. Pahl, E. B. Traenckner, C. Mueller-Dieckmann, D. Farahifar, B. Rossi, P. Auberger, P. A. Baeuerle, and J. F. Peyron.** 1996. Tyrosine phosphorylation of I kappa B-alpha activates NF-kappa B without proteolytic degradation of I kappa B-alpha. Cell **86:**787–798.
11. **Letunic, I., L. Goodstadt, N. J. Dickens, T. Doerks, J. Schultz, R. Mott, F. Ciccarelli, R. R. Copley, C. P. Ponting, and P. Bork.** 2002. Recent improvements to the SMART domain-based sequence annotation resource. Nucleic Acids Res. **30:**242–244.
12. **Livolsi, A., V. Busuttil, V. Imbert, R. T. Abraham, and J. F. Peyron.** 2001. Tyrosine phosphorylation-dependent activation of NF-kappa B. Requirement for p56 LCK and ZAP-70 protein tyrosine kinases. Eur. J. Biochem. **268:**1508–1515.
13. **Marck, C.** 1988. "DNA Strider": a "C" program for the fast analysis of DNA and protein sequences on the Apple Macintosh family of computers. Nucleic Acids Res. **16:**1829–1836.
14. **Messud-Petit, F., J. Gelfi, M. Delverdier, M. F. Amardeilh, R. Py, G. Sutter, and S. Bertagnoli.** 1998. Serp2, an inhibitor of the interleukin-1β-converting enzyme, is critical in the pathobiology of myxoma virus. J. Virol. **72:**7830–7839.
15. **Mosavi, L. K., D. L. Minor, Jr., and Z. Y. Peng.** 2002. Consensus-derived structural determinants of the ankyrin repeat motif. Proc. Natl. Acad. Sci. USA **99:**16029–16034.
16. **Neilan, J. G., Z. Lu, G. F. Kutish, L. Zsak, T. L. Lewis, and D. L. Rock.** 1997. A conserved African swine fever virus IkappaB homolog, 5EL, is nonessential for growth in vitro and virulence in domestic swine. Virology **235:**377–385.
17. **Oie, K. L., and D. J. Pickup.** 2001. Cowpox virus and other members of the orthopoxvirus genus interfere with the regulation of NF-kappaB activation. Virology **288:**175–187.
18. **Petit, F., S. Bertagnoli, J. Gelfi, F. Fassy, C. Boucraut-Baralon, and A. Milon.** 1996. Characterization of a myxoma virus-encoded serpin-like protein with activity against interleukin-1β-converting enzyme. J. Virol. **70:**5860–5866.
19. **Powell, P. P., L. K. Dixon, and R. M. Parkhouse.** 1996. An IκB homolog encoded by African swine fever virus provides a novel mechanism for down-regulation of proinflammatory cytokine responses in host macrophages. J. Virol. **70:**8527–8533.
20. **Revilla, Y., M. Callejo, J. M. Rodriguez, E. Culebras, M. L. Nogal, M. L. Salas, E. Vinuela, and M. Fresno.** 1998. Inhibition of nuclear factor kappaB activation by a virus-encoded IkappaB-like protein. J. Biol. Chem. **273:**5405–5411.
21. **Sachdev, S., A. Hoffmann, and M. Hannink.** 1998. Nuclear localization of IκBα is mediated by the second ankyrin repeat: the IκBα ankyrin repeats define a novel class of *cis*-acting nuclear import sequences. Mol. Cell. Biol. **18:**2524–2534.
22. **Santoro, M. G., A. Rossi, and C. Amici.** 2003. NF-kappaB and virus infection: who controls whom. EMBO J. **22:**2552–2560.
23. **Schultz, J., F. Milpetz, P. Bork, and C. P. Ponting.** 1998. SMART, a simple modular architecture research tool: identification of signaling domains. Proc. Natl. Acad. Sci. USA **95:**5857–5864.
24. **Sedgwick, S. G., and S. J. Smerdon.** 1999. The ankyrin repeat: a diversity of interactions on a common structural framework. Trends Biochem. Sci. **24:**311–316.
25. **Shchelkunov, S. N., V. M. Blinov, and L. S. Sandakhchiev.** 1993. Ankyrin-like proteins of variola and vaccinia viruses. FEBS Lett. **319:**163–165.
26. **Shchelkunov, S. N., P. F. Safronov, A. V. Totmenin, N. A. Petrov, O. I. Ryazankina, V. V. Gutorov, and G. J. Kotwal.** 1998. The genomic sequence analysis of the left and right species-specific terminal region of a cowpox virus strain reveals unique sequences and a cluster of intact ORFs for immunomodulatory and host range proteins. Virology **243:**432–460.
27. **Simeonidis, S., D. Stauber, G. Chen, W. A. Hendrickson, and D. Thanos.** 1999. Mechanisms by which IkappaB proteins control NF-kappaB activity. Proc. Natl. Acad. Sci. USA **96:**49–54.
28. **Tait, S. W., E. B. Reid, D. R. Greaves, T. E. Wileman, and P. P. Powell.** 2000. Mechanism of inactivation of NF-kappa B by a viral homologue of I kappa B alpha. Signal-induced release of I kappa B alpha results in binding of the viral homologue to NF-kappa B. J. Biol. Chem. **275:**34656–34664.
29. **Turpin, P., R. T. Hay, and C. Dargemont.** 1999. Characterization of IkappaBalpha nuclear import pathway. J. Biol. Chem. **274:**6804–6812.
30. **Upton, C., J. L. Macen, D. S. Wishart, and G. McFadden.** 1990. Myxoma virus and malignant rabbit fibroma virus encode a serpin-like protein important for virus virulence. Virology **179:**618–631.
31. **Willer, D. O., G. McFadden, and D. H. Evans.** 1999. The complete genome sequence of Shope (rabbit) fibroma virus. Virology **264:**319–343.